

## Metasurface of aluminum nanocylinders to enhance the chemiluminescence of luminol

© D.R. Dadadzhanov, A.V. Palekhova, T.A. Vartanyan

International research and educational center for physics of nanostructures, ITMO University, 197101 Saint-Petersburg, Russia

e-mail: Tigran.Vartanyan@mail.ru

Received December 8, 2023

Revised December 8, 2023

Accepted December 11, 2023

As a result of numerical modeling, the parameters of a square lattice of aluminum nanocylinders were found, which ensures the maximum enhancement of luminol chemiluminescence at a wavelength of 430 nm. The period of the lattice formed by aluminum nanocylinders and the radius of the nanocylinders were varied at a constant height of 20 nm. The enhancement factor was averaged over a layer of an aqueous solution of the analyte and luminol covering the nanocylinders. While the maximum enhancement factor for chemiluminophore molecules located near the surface of nanocylinders exceeds a thousand, the enhancement value averaged over the reaction mixture layer under optimal conditions was 3.2.

**Keywords:** plasmon resonance, aluminum nanoparticles, chemiluminescence, luminol, modeling.

DOI: 10.61011/EOS.2023.12.58186.5850-23

### Introduction

Chemiluminescence is widely used in various chemical and biological sensors. Sensors relying on the emission of light by chemiluminophore molecules excited as a result of an exothermic chemical reaction have high sensitivity and selectivity. This led to their application in fields such as medical diagnostics [1,2], pharmaceuticals [3], and reactive oxygen intermediates (ROI) [4,5] detection. Sensors based on chemiluminescence have an unquestionable advantage in the non-necessity of an external source of optical excitation, which significantly complicates the design and increases the cost of devices relying on other optical phenomena (in particular, photoluminescence). The disadvantages of chemiluminescence-based devices include the low intensity of chemiluminescence radiation, which makes detection of small concentrations of analytes difficult. Therefore, the search for ways to increase the intensity of chemiluminescence is an urgent task.

One promising approach to increasing the chemiluminescence intensity is the use of metallic nanoparticles. It is known that nanoparticles featuring plasmon resonances can act as nanoantennas and, due to the Purcell effect, increase the rate of radiative decay of chemiluminophores, which, in turn, leads to an increase in the quantum yield of chemiluminescence [6,7]. It has been demonstrated earlier that chemiluminescence of one of the most popular luminophores — luminol — may be enhanced by adding colloidal silver and gold nanoparticles [8] to the reaction mixture. Unfortunately, the results obtained with colloidal nanoparticles are hard to reproduce due to the uncertainty in the size and shape of synthesized nanoparticles. Even a slight violation of the synthesis conditions leads to a large scatter of nanoparticles in size and shape and, as a

consequence, their departure from resonance with emitting chemiluminophore molecules. Much greater accuracy and reproducibility of nanoparticle sizes and shapes can be obtained by electron beam lithography [9]. In the present work, we discuss the design of such a periodic structure of metallic nanoparticles that, on the one hand, can be created by electron beam lithography and, on the other hand, interacts resonantly with luminol and enhances its chemiluminescence. Aluminum [10], which is stable in aqueous environment due to the natural formation of a thin oxide film with barrier properties on the surface, was chosen as the nanoparticle material. As calculations have shown, a correct choice of the size and location of aluminum nanocylinders on the substrate allows for an overlap of the plasmon resonance band with the chemiluminescence spectrum of the chemiluminophore, which provides effective electromagnetic coupling of emitting molecules with plasmonic nanoparticles and a corresponding acceleration of radiation processes.

### Parameters of the computational model of the metasurface of metallic nanocylinders

The search for the optimal metasurface configuration to enhance luminol chemiluminescence was conducted among periodic structures in the form of a square lattice of straight circular cylinders made of aluminum. The dependence of the spectral position and intensity of the plasmon resonance of the periodic structure (see Fig. 1) on the radius of cylinders and the lattice period at a constant cylinder height of 20 nm was studied. Fused quartz SiO<sub>2</sub> with a refraction index of 1.46 was chosen as the substrate and, in accordance with the intended use, it was assumed that the

system was immersed in an aqueous solution of analyte and luminol. In view of the smallness of reagent concentrations, the refraction index of this solution was assumed to be equal to that of water (1.33). The dielectric permittivity of aluminum was taken from [11]. The position of the plasmon resonance and its influence on the emission of chemiluminescence molecules was evaluated according to the results of electrodynamic calculations performed using the COMSOL Multiphysics software package. Floquet-type boundary conditions were used to model a periodic array of nanoparticles.

### Calculated transmission and reflection spectra of a metasurface of aluminum nanoparticles

The initial selection of geometric parameters of the metasurface was performed using the reflection and transmission spectra shown in Fig. 2. Aluminum nanocylinders formed a square lattice with a period of 250 nm. The sharp decrease in transmittance ( $T$ ) and increase in reflection ( $R$ ) at certain wavelengths is attributed to the excitation of plasmon resonance in aluminum nanocylinders at these wavelengths. Absorption  $A$ , which can be calculated as  $A = 100 - T - R$ , also increases at the same wavelengths. When the radius of nanocylinders changes from 30 to 60 nm, the plasmon resonance band broadens, and its maximum shifts monotonically toward longer wavelengths. This allows us to achieve a significant overlap with the chemiluminescence spectrum of luminol, the maximum of which is marked in Fig. 2 by a vertical dashed line, at a nanocylinder radius of 40 nm (line 3 in Fig. 2). Since the greatest increase in chemiluminescence intensity due to the Purcell effect occurs when the plasmon resonance band coincides with the chemiluminescence band, it seemed reasonable to specify the metasurface parameters using the

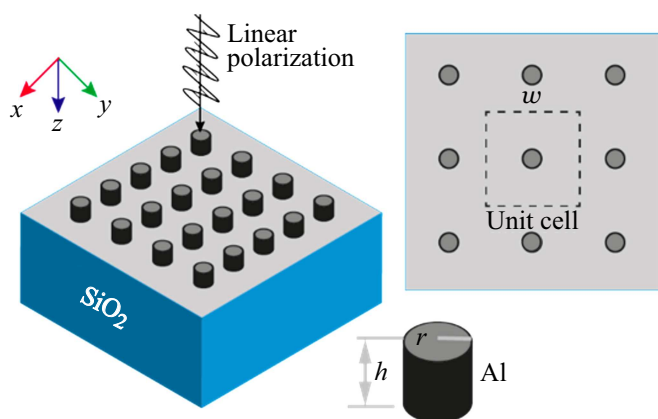


**Figure 1.** Model of a metasurface of metallic nanocylinders forming a square lattice on a quartz substrate. Experimental values of the optical constants of aluminum were used in simulations. The refraction index of the medium covering the structure was assumed to be equal to the refraction index of water.

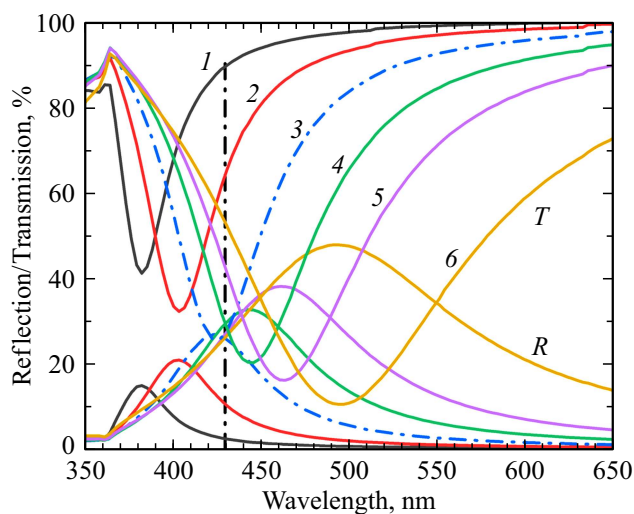


**Figure 2.** Reflectance ( $R$ ) and transmittance ( $T$ ) spectra of an aluminum metasurface of nanocylinders with different radii: 1 — 30 nm, 2 — 35 nm, 3 — 40 nm, 4 — 45 nm, 5 — 50 nm, and 6 — 60 nm. Dash-and-dot curves represent the transmission and reflection spectra of the metasurface formed by aluminum nanocylinders with a radius of 40 nm. They are highlighted as the ones being the closest to the chemiluminescence spectrum of luminol the maximum of which is marked by a vertical dashed line.

experimentally obtained chemiluminescence spectrum of luminol.

### Experimental chemiluminescence spectrum of luminol

Chemiluminescence was observed when a  $10^{-4}$  M luminol solution was mixed with a 0.05% sodium hypochlorite solution acting as an oxidizing agent. Since the chemiluminescence signal-to-noise ratio was low in a neutral medium (pH=7), the chemiluminescence spectrum of luminol shown in Fig. 3 was measured in an alkaline medium at pH=12. By interpolation of the data presented in Fig. 2, it was determined that the maximum of the absorption spectrum of the metasurface composed of aluminum nanocylinders with a radius of 41.5 nm should coincide with the maximum of luminol chemiluminescence at a wavelength of 430 nm. The calculation results shown in Fig. 3, *a* confirm the excellent overlap of the plasmon resonance spectrum of the metasurface composed of aluminum nanocylinders with the chemiluminescence spectrum of luminol.

### Calculation of the maximum and cell-averaged near-field plasmonic enhancement

Despite the fact that the absorption spectra allow us to determine the spectral position of localized plasmon

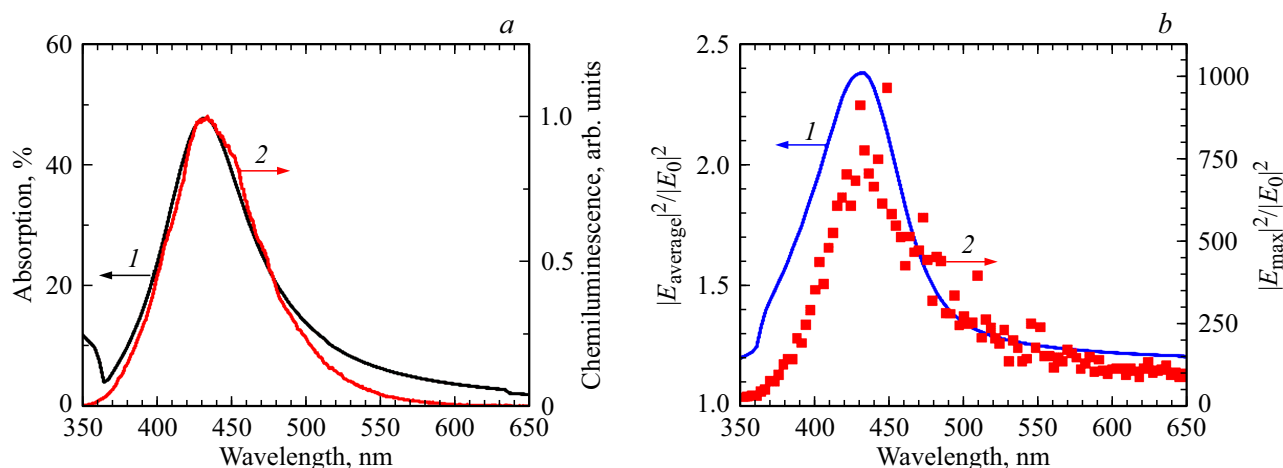


**Figure 3.** (a) Overlap of the absorption spectrum of the metasurface composed of aluminum nanocylinders with a radius of 41.5 nm (1) with the chemiluminescence spectrum of luminol (2). (b) Average value of field enhancement in the lattice cell of a periodic structure with a height of 40 nm from which the volume occupied by the metallic nanocylinder is excluded (1) and maximum field enhancement outside the nanocylinder (2).

resonance, a more accurate tuning of the metasurface parameters should be performed based on the averaged Purcell factor, which, in turn, can be estimated by the value of the local electric field enhancement upon excitation of the plasmon resonance by external radiation. As was shown in [12], under resonant conditions, the specific type of external excitation is immaterial, so that radiation of a molecule near a plasmonic nanoparticle can be replaced by a plane electromagnetic wave with amplitude  $E_0$  in the calculation of the gain factor.

Figure 3, b shows the results of calculation of the ratio of the squared modulus of local field amplitude  $E$  to the squared modulus of the amplitude of an incident plane linearly polarized wave  $|E|^2/|E_0|^2$ : line 1 is the result of averaging this ratio over the lattice cell of a periodic structure with a height of 40 nm from which the volume occupied by the metallic nanocylinder is excluded, and line 2 represents the maximum value of this ratio. Since the maximum gain factor reaches 1000 and is many times higher than the average gain, which is limited to 2.5, it is of interest to see the distribution of gain over the space within which an emitting chemiluminophore molecule can be located.

Figure 4 shows maps of the  $|E|^2/|E_0|^2$  field enhancement distribution at a wavelength of 430 nm corresponding to the luminol chemiluminescence maximum in two planes running parallel to the substrate surface ( $z = 0$ ) at heights equal to half the height of nanocylinders  $z = 10$  nm (Fig. 4, a) and to their full height  $z = 20$  nm (Fig. 4, b). The enhancement is large near the lateral surface of nanocylinders and decreases rapidly when moving away from it. In connection with this, the possibility of altering the period of the structure so as to minimize the useless volume between nanoparticles, where the field enhancement is small, without violating the excitation conditions of the plasmon resonance

is of interest. The shift of the resonant wavelength due to electromagnetic coupling between neighboring nanocylinders should be compensated by changing the radius of nanocylinders.

Figure 5 shows the results of calculation of the near-field enhancement averaged over a 40-nm-thick water layer that covers aluminum nanocylinders. The wavelength of incident radiation corresponded to the luminol chemiluminescence maximum of 430 nm, and the radius of nanocylinders and the period of the square lattice were varied. The average field enhancement reaches a maximum of 3.2 times at a lattice period of 295 nm and a nanocylinder radius of 35 nm.

## Discussion of the calculation results

As was mentioned in the introductory section, the operation of many chemical and biological sensors is based on luminol chemiluminescence. Despite the wide variety of options for detection of various analytes offered by luminol chemiluminescence [13], the key stage of the process leading to optical emission is the oxidation of luminol by one or another reactive oxygen intermediate. It is at this stage that the products of a chemical reaction are in an excited state, which, with a certain probability, transitions to the ground state by emitting a quantum of light. Since the process of nonradiative deactivation of the excited state of a molecule competes with the emission of light quanta, the intensity of chemiluminescence is determined by the ratio of the rates of radiative and nonradiative deactivation of excited products of the luminol oxidation reaction. Due to the fact that the rate of nonradiative transitions is much higher than the radiative transition rate, the quantum yield of chemiluminescence is small, but can be increased by increasing the rate of radiative transitions. The realization of this possibility by placing an emitting molecule near a

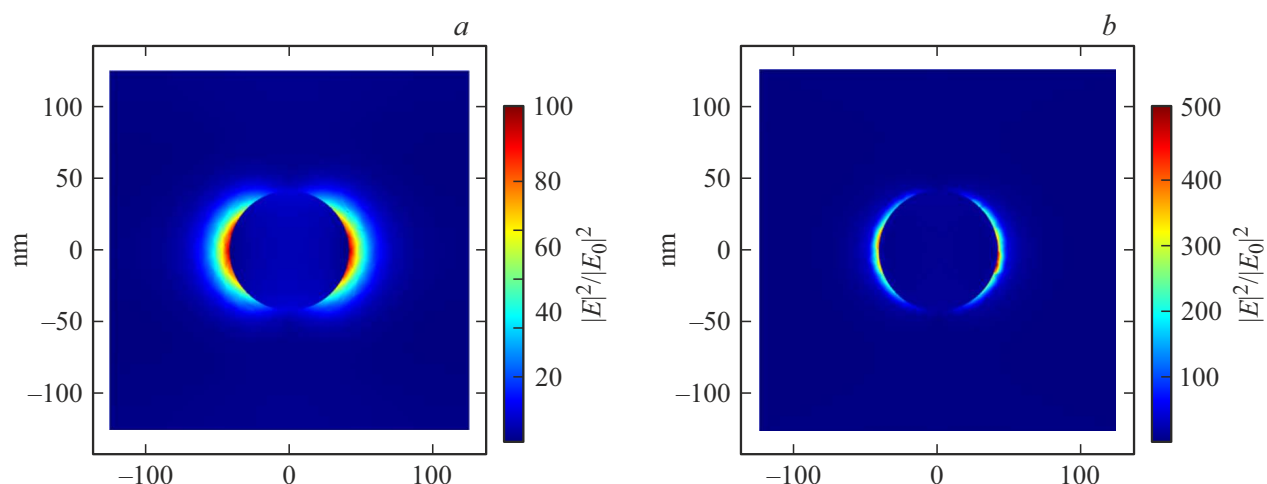


**Figure 4.** Distribution maps of local field enhancement  $|E|^2/|E_0|^2$  at a wavelength of 430 nm within the lattice cell of a periodic structure of aluminum nanocylinders with a height of 20 nm at distances  $z = 10$  (a) and 20 nm (b) from the substrate surface.

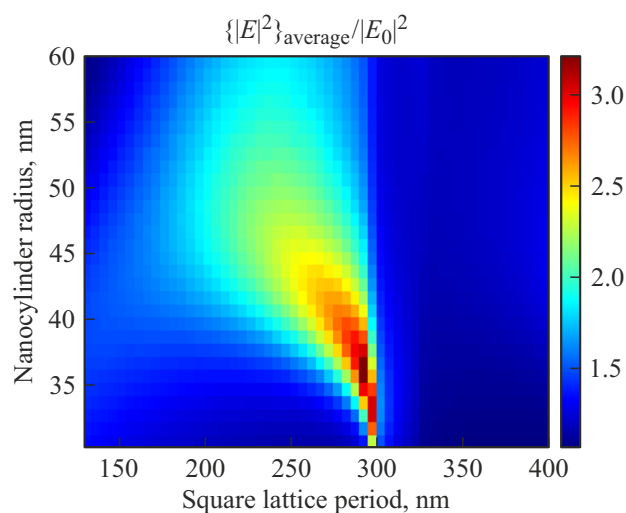


**Figure 5.** Average electric field enhancement in a periodic lattice of aluminum nanocylinders as a function of the lattice period and radius of nanocylinders at their fixed height  $h = 20$  nm. Averaging was performed over a 40-nm-thick layer of water simulating the analyte solution.

metallic nanoparticle featuring a localized surface plasmon resonance has been termed metal-enhanced chemiluminescence [14]. In the present work, we have elucidated the feasibility of chemiluminescence enhancement of luminol with a metasurface of aluminum nanocylinders that can be created by electron beam lithography. As a result of extensive numerical simulations, such parameters of the square lattice of aluminum nanocylinders at which the local field enhancement factor averaged over the lattice cell of the periodic structure reaches its maximum have been found. According to [12], these same parameters correspond to the maximum increase in the radiative transition rate and,

consequently, the maximum increase in chemiluminescence intensity.

## Conclusion

The use of a metasurface formed by a periodic lattice of aluminum nanocylinders makes it possible to realize the process of metal-enhanced chemiluminescence. At optimal geometrical parameters, such a metasurface provides 3-fold acceleration of radiation processes and a corresponding enhancement of chemiluminescence intensity.

## Funding

This study was supported by grant No. 23-72-00045 from the Russian Science Foundation, <https://rscf.ru/project/23-72-00045/>.

## Conflict of interest

The authors declare that they have no conflict of interest.

## References

- [1] I. Bronstein, C.E.M. Olesen. *Molecular Methods for Virus Detection*, ed. by D.L. Wiedbrauk, D.H. Farkas (Elsevier, 1995), p. 147–174. DOI: 10.1016/B978-012748920-9/50008-X
- [2] L. Cinquanta, D.E. Fontana, N. Bizzaro. *Autoim. Highlights*, **8** (1), 9 (2017). DOI: 10.1007/s13317-017-0097-2
- [3] B. Gómez-Taylor, M. Palomeque, J.V. García Mateo, J. Martínez Calatayud. *J. Pharm. Biomed. Anal.*, **41** (2), 347–357 (2021). DOI: 10.1016/j.jpba.2005.11.040
- [4] W. Yu, L. Zhao. *TrAC Trends in Analytical Chemistry*, **136**, 116197 (2021). DOI: 10.1016/j.trac.2021.116197
- [5] L. Liu, C. Dahlgren, H. Elwing, H. Lundqvist. *J. Immunol. Methods*, **192** (1?2), 173–178 (1996). DOI: 10.1016/0022-1759(96)00049-X

- [6] D.R. Dadadzhanov, I.A. Gladskikh, M.A. Baranov, T. A. Vartanyan, A. Karabchevsky. *Sens. and Act. B: Chem.* **333**, 129453 (2021). DOI: 10.1016/j.snb.2021.129453
- [7] H. Chen, F. Gao, R. He, D. Cui. *J. Coll. Interf. Sci.*, **315** (1), 158–163 (2007). DOI: 10.1016/j.jcis.2007.06.052
- [8] A. Karabchevsky, A. Mosayyebi, A.V. Kavokin. *Light: Sci. Appl.*, **5** (11), e16164–e16164 (2016). DOI: 10.1038/lsa.2016.164
- [9] J. Wang, J. Du. *Appl. Sci.*, **6** (9), 239 (2016). DOI: 10.3390/app6090239
- [10] J. Hu, L. Chen, Z. Lian, M. Cao, H. Li, W. Sun, N. Tong, H. Zeng. *J. Phys. Chem. C.*, **116** (29), 15584–15590 (2012). DOI: 10.1021/jp305844g
- [11] P.B. Johnson, R.W. Christy. *Phys. Rev. B.*, **6** (12), 4370–4379 (1972). DOI: 10.1103/PhysRevB.6.4370
- [12] A.E. Krasnok, A. P. Slobozhanyuk, C.R. Simovski, S.A. Tretyakov, A.N. Poddubny, A.E. Miroschnichenko, Yu.S. Kivshar, P.A. Belov. *Sci. Rep.*, **5**, 12956 (2015). DOI: 10.1038/srep12956
- [13] D.A. Gorbenkoa, P.V. Filatova, D.R. Dadadzhanov, K.K. Kirichek, M.Yu. Berezovskaya, T.A. Vartanyan. *Proc. SPIE*, **12663**, 1266307 (2023). DOI: 10.1117/12.2676447
- [14] K. Aslan, C.D. Geddes. *Chem. Soc. Rev.*, **38**, 2556 (2009). DOI: 10.1039/B807498B

*Translated by D.Safin*